

**A laser flash photolysis kinetics study of the reaction  $\text{OH} + \text{H}_2\text{O}_2 \rightarrow \text{HO}_2 + \text{H}_2\text{O}$** 

P. H. Wine, D. H. Semmes, and A. R. Ravishankara

Citation: *The Journal of Chemical Physics* **75**, 4390 (1981); doi: 10.1063/1.442602

View online: <http://dx.doi.org/10.1063/1.442602>

View Table of Contents: <http://scitation.aip.org/content/aip/journal/jcp/75/9?ver=pdfcov>

Published by the [AIP Publishing](#)

---

**Articles you may be interested in**

[Laser flash photolysis studies of radical-radical reaction kinetics: The  \$\text{O}\(^3\text{P}\) + \text{BrO}\$  reaction](#)

*J. Chem. Phys.* **102**, 4131 (1995); 10.1063/1.468541

[A comparative study of the reaction dynamics of the  \$\text{O}\(^3\text{P}\) + \text{H}\_2 \rightarrow \text{OH} + \text{H}\$  reaction on several potential energy surfaces. III. Collinear exact quantum transmission coefficient correction to transition state theory](#)

*J. Chem. Phys.* **76**, 3583 (1982); 10.1063/1.443395

[A comparative study of the reaction dynamics of several potential energy surfaces for  \$\text{O}\(^3\text{P}\) + \text{H}\_2 \rightarrow \text{OH} + \text{H}\$ . II. Collinear exact quantum and quasiclassical reaction probabilities](#)

*J. Chem. Phys.* **76**, 3563 (1982); 10.1063/1.443394

[Kinetics of the reaction  \$\text{OH} + \text{H}\_2\text{O}\_2 \rightarrow \text{HO}\_2 + \text{H}\_2\text{O}\$](#)

*J. Chem. Phys.* **73**, 1286 (1980); 10.1063/1.440240

[Flash photolysisresonance fluorescence kinetics study: Temperature dependence of the reactions  \$\text{OH} + \text{CO} \rightarrow \text{CO}\_2 + \text{H}\$  and  \$\text{OH} + \text{CH}\_4 \rightarrow \text{H}\_2\text{O} + \text{CH}\_3\$](#)

*J. Chem. Phys.* **61**, 2213 (1974); 10.1063/1.1682293

---



# A laser flash photolysis kinetics study of the reaction $\text{OH} + \text{H}_2\text{O}_2 \rightarrow \text{HO}_2 + \text{H}_2\text{O}$

P. H. Wine, D. H. Semmes, and A. R. Ravishankara

Molecular Sciences Group, Engineering Experiment Station, Georgia Institute of Technology, Atlanta, Georgia 30332

(Received 28 May 1981; accepted 29 June 1981)

Absolute rate constants for the reaction  $\text{OH} + \text{H}_2\text{O}_2 \xrightarrow{k_1} \text{HO}_2 + \text{H}_2\text{O}$  are reported as a function of temperature over the range  $273 < T < 410$  K. OH radicals were produced by 266 nm laser photolysis of  $\text{H}_2\text{O}_2$  and detected by resonance fluorescence.  $\text{H}_2\text{O}_2$  concentrations were determined *in situ* in the slow flow system by UV photometry. An unweighted linear least squares analysis of the  $\ln k_1$  vs  $T^{-1}$  data gives the Arrhenius expression  $k_1 = (3.7 \pm 0.6) \times 10^{-12} \exp[-(260 \pm 50)/T] \text{ cm}^3 \text{ molecule}^{-1} \text{ s}^{-1}$ , where the errors are  $2\sigma$  and refer to precision only. The estimated accuracy of each  $k_1(T)$  is  $\pm 20\%$ . Our results confirm the findings of two recent discharge flow-resonance fluorescence studies that the title reaction is considerably faster, particularly at temperatures below 300 K, than all earlier studies had indicated.

## INTRODUCTION

$\text{H}_2\text{O}_2$  is an important reservoir for the reactive free radicals OH and  $\text{HO}_2$  ( $\text{HO}_x$ ) in both the stratosphere and the troposphere. In the stratosphere,  $\text{HO}_x$  directly catalyzes the destruction of  $\text{O}_3$  and also participates in a complex reaction scheme which controls the efficiency of other catalytic cycles involving  $\text{NO}_x$  and chlorine. One of the important  $\text{H}_2\text{O}_2$  destruction mechanisms in the atmosphere is the reaction



The extent to which Reaction (1) competes with solar photolysis affects both the  $\text{HO}_x$  concentration and the OH/ $\text{HO}_2$  ratio in the stratosphere. In the troposphere, Reaction (1) and rainout are the important  $\text{H}_2\text{O}_2$  removal processes. Hence, knowledge of  $k_1$  is needed to assess the role of  $\text{H}_2\text{O}_2$  in such diverse processes as acid rain and hydrocarbon degradation.

Early measurements of  $k_1^{1-5}$  yielded rate constants at 298 K which ranged from  $0.62$ – $1.2 \times 10^{-12} \text{ cm}^3 \text{ molecule}^{-1} \text{ s}^{-1}$ . Based on these results and two studies of the temperature dependence of  $k_1$ ,<sup>1,4</sup> the expression  $k_1 = 1.0 \times 10^{-11} \exp(-750/T)$  was recommended for atmospheric modeling.<sup>6</sup> Two subsequent studies,<sup>7,8</sup> both of which employed the discharge flow-resonance fluorescence technique (DF-RF) are in agreement that  $k_1$  is a factor of 2 faster at 298 K and a factor of 3–5 faster at stratospheric temperatures than the previous results suggested. The implications of these new kinetic data for atmospheric chemistry are substantial. Hence, confirmation of the new results by a different but equally reliable experimental technique is desirable. The present investigation was undertaken to provide such confirmation. Features of the experimental technique which make it particularly suitable for studying Reaction (1) include (a) production of OH in the absence of other reactive radicals, (b) direct measurement of the  $\text{H}_2\text{O}_2$  concentration at the entrance and exit of the reactor, and (c) isolation of the reaction zone from the walls of the reactor. Our results are in good agreement with the two recent DR-RF studies.<sup>7,8</sup>

## EXPERIMENTAL

The apparatus used in this study is similar to that employed in our laboratory in other recent investigations of OH reaction kinetics.<sup>9,10</sup> Some modifications were required to facilitate the handling of  $\text{H}_2\text{O}_2$  and measurement of the  $\text{H}_2\text{O}_2$  concentration.

The jacketed reaction cell was constructed of Pyrex and had an internal volume of  $\sim 150 \text{ cm}^3$ . Quartz optics were attached to the cell with Viton o-rings. The cell was maintained at a known constant temperature by circulating an ethylene glycol-water mixture through the outer jacket. OH radicals were produced by pulsed laser photolysis of  $\text{H}_2\text{O}_2$  at 266 nm (fourth harmonic, Nd:YAG laser). An OH resonance lamp perpendicular to the photolysis source excited resonance fluorescence in the 0–0 band of the  $A^2\Sigma^+ - X^2\Pi$  system; this fluorescence was detected perpendicular to both the photolysis beam and the resonance fluorescence excitation beam by a photomultiplier fitted with an interference filter (309.5 nm peak transmission, 10 nm FWHM). Signals were obtained by photon counting and then fed into a signal averager operating in the multichannel scaling mode. For each decay rate measured, sufficient flashes (10–2000 depending on signal strength) were averaged to obtain a well defined temporal profile over at least a factor of 20 variation in [OH].

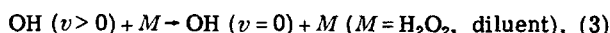
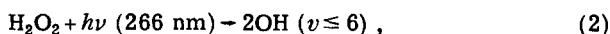
All experiments were carried out under "slow flow" conditions. Linear flow rates through the reactor ranged from  $5$ – $11 \text{ cm s}^{-1}$ . The laser repetition rate was 1 Hz in all experiments, so the flow rate was sufficiently fast to provide a fresh reaction mixture for each laser shot. Experiments were run at flow rates considerably faster than those employed in previous studies of OH reactions in order to minimize decomposition of  $\text{H}_2\text{O}_2$  in the reactor. The  $\text{H}_2\text{O}_2$ /diluent gas reaction mixture was generated by bubbling diluent through  $\text{H}_2\text{O}_2$  at 298 K and combining the mixture thus obtained with additional diluent gas before it entered the reaction cell. All components traversed by  $\text{H}_2\text{O}_2$  were Pyrex or Teflon with the exception of a few stainless steel fittings. As an extra precaution against decomposition, the needle valve

and flow meter in the  $\text{H}_2\text{O}_2$  line were positioned before the bubbler.

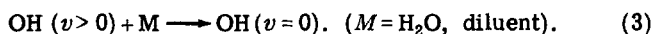
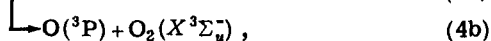
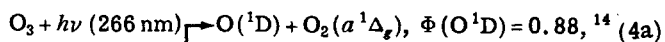
The concentration of  $\text{H}_2\text{O}_2$  in the mixture exiting (or in some cases entering) the reactor was directly measured (at 298 K) by absorption at 228.8 nm using a Cd lamp as the light source and a 151 cm absorption cell. The 228.8 nm line was isolated from other lamp emissions by a combination of a bandpass filter with peak transmission at 185 nm and a cell containing 600 Torr cm  $\text{CS}_2$ . The bandpass filter transmitted two lines, one at 228.8 nm and a weaker line at 214.4 nm; the 214.4 nm line was completely attenuated ( $> 99\%$ ) by the  $\text{CS}_2$  filter. Lamp emission transmitted by the filters and absorption cell was detected by a quartz envelope RCA-1P28 photomultiplier, and the anode current was measured by an electrometer. Before each run, the  $\text{H}_2\text{O}_2$  flow was shut off the absorption cell and the reactor were flushed with diluent gas, and the unattenuated light intensity  $I_0$  was measured.  $\text{H}_2\text{O}_2$  was then added and the attenuated light intensity  $I_0$  was monitored continuously during the experiment. After completion of the experiment, the absorption cell and reactor were again flushed and  $I_0$  re-measured. The  $\text{H}_2\text{O}_2$  absorption cross section, obtained by interpolation of the data of Molina and Molina,<sup>11</sup> was taken to be  $1.73 \times 10^{-19} \text{ cm}^2$  at 228.8 nm. Over the range of  $\text{H}_2\text{O}_2$  concentrations investigated, absorptions of 1–12% were measured. The precision of the  $\text{H}_2\text{O}_2$  concentration measurements was  $\sim 10\%$  for the highest concentrations measured and  $\sim 25\%$  for the lowest concentrations measured. In some preliminary experiments, absorption at 185.0 nm (Hg lamp) was employed to monitor  $\text{H}_2\text{O}_2$ . At 185.0 nm the  $\text{H}_2\text{O}_2$  absorption cross section is 4–5 times larger than at 228.8 nm. However, 228.8 nm was settled on as the monitoring wavelength of choice because (1) the absorption cross section is known more accurately at 228.8 nm than at 185.0 nm, and (2) the Cd lamp was found to be considerably more stable than the Hg lamp.

The diluent gases used in this study had the following stated purities:  $\text{He} \geq 99.999\%$ ,  $\text{SF}_6 \geq 99.99\%$ . They were used without purification.  $\text{H}_2\text{O}_2$ , obtained from FMC corporation, was 90% pure by weight. It was further concentrated by pumping for several hours at 273 K before use.  $\text{H}_2\text{O}$  was Baker Instra-Analyzed and was used without purification.  $\text{O}_3$  was prepared by passing ultra-high purity  $\text{O}_2$  through a commercial ozonator and storing on silica gel at 197 K. Before use, it was degassed at 77 K to remove  $\text{O}_2$ .

As mentioned above, OH radicals were produced by 266 nm laser photolysis of  $\text{H}_2\text{O}_2$ :



It is well established that reaction (2) is the dominant photolysis channel in the 266 nm wavelength region.<sup>12,13</sup> In order to measure the rate of OH removal in the absence of  $\text{H}_2\text{O}_2$ , a mixture containing 0.5 mTorr  $\text{O}_3$ , 60 mTorr  $\text{H}_2\text{O}$ , and diluent gas was photolyzed:



With  $[\text{OH}]_0 \sim 1 \times 10^{12} \text{ cm}^{-3}$ , reactions of OH with itself and with  $\text{O}_3$  were of negligible importance; the OH decay was dominated by diffusion from the field of view of the detector and reaction with background impurities.

The range of  $k'$  values measured in this study (excluding those obtained in the absence of  $\text{H}_2\text{O}_2$ ) are in the range  $749\text{--}6390 \text{ s}^{-1}$ —about an order of magnitude faster than is typical of flash photolysis–resonance fluorescence experiments. This large deviation from normal operating conditions was dictated by our desire to employ reaction mixtures with  $\text{H}_2\text{O}_2$  concentrations which were directly measurable by absorption. Measurements of pseudo-first-order rate constants significantly faster than  $6390 \text{ s}^{-1}$  was not feasible because fluorescence excited in the reactor walls and optical filters by scattered laser radiation ( $=$  flash) was similar in signal strength (at  $t = 0$ ) to the OH resonance fluorescence and decayed with a lifetime of  $\sim 40 \mu\text{s}$ . The flash signal was always negligible in intensity compared to the resonance fluorescence signal for all  $t > 150 \mu\text{s}$  following the laser shot, so accurate decay rates could be obtained by simply excluding the first few channels of data from the analysis.

The laser photon flux transmitted through the reaction cell was  $\sim 5 \text{ mJ cm}^{-2}$  from which it can be calculated that for all experiments employing Reaction (2) as the sole OH production mechanism, the  $\text{H}_2\text{O}_2$  concentration exceeded the initial OH concentration by about a factor of 3000. Therefore, if secondary reactions which remove or produce OH are suppressed, the OH temporal profile should obey simple first order kinetics:

$$\ln \{[\text{OH}]_0/[\text{OH}]_t\} = (k_1 [\text{H}_2\text{O}_2] + k_d)t \equiv k't, \quad (I)$$

where  $k_d$  is the first order rate constant for loss of OH in the absence of  $\text{H}_2\text{O}_2$  and  $k'$  is the measured pseudo-first-order rate constant. The bimolecular rate constant  $k_1$  is determined from the slope of a  $k'$  vs  $[\text{H}_2\text{O}_2]$  plot. Observation of OH temporal profiles which are exponential [i.e., obey Eq. (I)], a linear dependence of  $k'$  on  $[\text{H}_2\text{O}_2]$ , and invariance of  $k_1$  to variations in  $[\text{OH}]_0$  serve as proof that the OH temporal profile is controlled by Reaction (1). Because  $\text{H}_2\text{O}_2$  readily undergoes heterogeneous decomposition, validation of the  $k_1$  determination also requires experimental verification that the  $\text{H}_2\text{O}_2$  concentration in the reaction zone is known.

## RESULTS AND DISCUSSION

The kinetics of Reaction (1) were investigated over the temperature range 273–410 K. Experiments at temperatures below 273 K were not possible due to the low vapor pressure of  $\text{H}_2\text{O}_2$ . Thermal decomposition of  $\text{H}_2\text{O}_2$  prohibited rate constant determinations at temperatures above 410 K. Exponential OH decays, typified by the data shown in Fig. 1, were observed under all experimental conditions investigated.

In most experiments, the reaction mixture flowed through the absorption cell after exiting the reactor. To

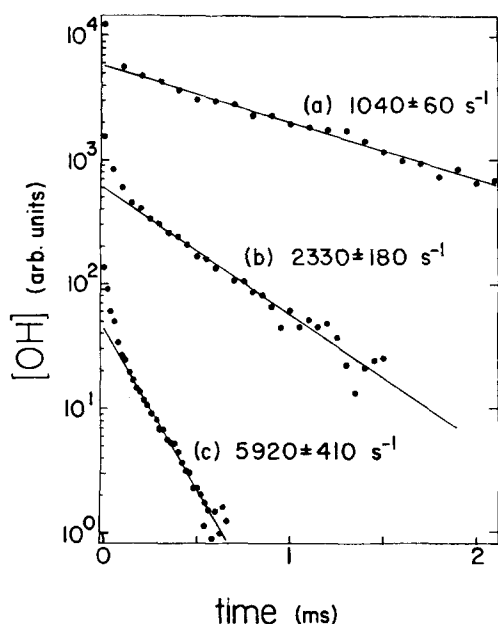


FIG. 1. Typical OH temporal profiles observed following 266 nm laser photolysis of  $\text{H}_2\text{O}_2/\text{He}$  mixtures. Experimental conditions:  $T=332\text{ K}$ ;  $P=100\text{ Torr (He)}$ ;  $[\text{H}_2\text{O}_2]$  in units of  $10^{15}\text{ molecules cm}^{-3}$  = (a) 0.52, (b) 1.45, (c) 3.4; Number of laser shots averaged = (a) 1200, (b) 1300, (c) 1600. Solid lines are obtained from linear least squares analyses of all data for  $t > 100\text{ }\mu\text{s}$ .  $k' \pm 2\sigma$  values obtained from the least squares analyses are given in the figure. Data from  $t \leq 100\text{ }\mu\text{s}$  were ignored because they contained a significant contribution from fluorescence excited in the reactor walls and optical filters by the photolysis laser.

check for the possibility that the  $\text{H}_2\text{O}_2$  concentration measured in the absorption cell was not identical to that present in the reaction zone, rate constants were determined at 298 and 410 K with the reaction mixture flowing through the absorption cell before entering the reactor. At 298 K, the measured  $k_1$  was independent of the position of the absorption cell. However, at 410 K the data obtained with the absorption cell at the entrance to the reactor displayed a somewhat nonlinear  $k'$  vs  $[\text{H}_2\text{O}_2]$  dependence while the data obtained with the absorption cell at the reactor exit gave a linear  $k'$  vs  $[\text{H}_2\text{O}_2]$  dependence (Fig. 2). This observation suggests that thermal decomposition of  $\text{H}_2\text{O}_2$  in the reactor was occurring at 410 K. As the reaction mixture flowed through the reactor, about 90% of the heated region was traversed prior to the reaction zone. For this reason, the  $k_1$  value obtained with the absorption cell at the reactor exit was expected to be minimally affected by thermal decomposition. Experimental verification for this hypothesis was obtained by demonstrating that with the absorption cell at the reactor exit, a factor of 2 increase in the linear flow rate through the reactor had no measurable effect on  $k_1$ .

Since radicals other than OH are not produced in significant quantities by the photoflash, the only radical-radical reactions which could affect the OH temporal profile are



Reaction (6) is much too slow to be important under the experimental conditions of low  $[\text{OH}]_0$  and fast  $k'$  which were employed. The rate constant for Reaction (7) is currently the subject of controversy but is not believed to be faster than  $1.1 \times 10^{-10}\text{ cm}^3\text{ molecule}^{-1}\text{ s}^{-1}$ ; calculations employing this maximum  $k_7$  suggest that under our experimental conditions Reaction (7) could contribute to the OH temporal profile after greater than 90% of OH was converted to  $\text{HO}_2$ . Because significant variations in laser intensity were not feasible, an alternate procedure was employed to check for interference from Reaction (7). This procedure involved addition of small amounts of  $\text{O}_3$  to the  $\text{H}_2\text{O}_2/\text{He}$  reaction mixture. With  $\text{O}_3$  present, OH is produced not only by Reaction (2), but also by the sequence of Reaction (6a) followed by



The rate constant for Reaction (8) is gas kinetic.<sup>15</sup> Hence, OH production via Reaction (8) was very fast compared to the rate of OH removal. With sufficient  $\text{O}_3$  added to increase  $[\text{OH}]_0$  by factors of 3–9 and also provide a large  $[\text{HO}_2]_0$ , the OH temporal profiles were found to be exponential and lie on the same  $k'$  vs  $[\text{H}_2\text{O}_2]$  line as those determined without added  $\text{O}_3$  (Figs. 2 and 3), thus demonstrating that Reaction (7) was not a kinetic complication. The use of Reaction (8) as an additional OH source also results in production of some  $\text{O}(^3\text{P})$  via Reaction (4b) and the reaction

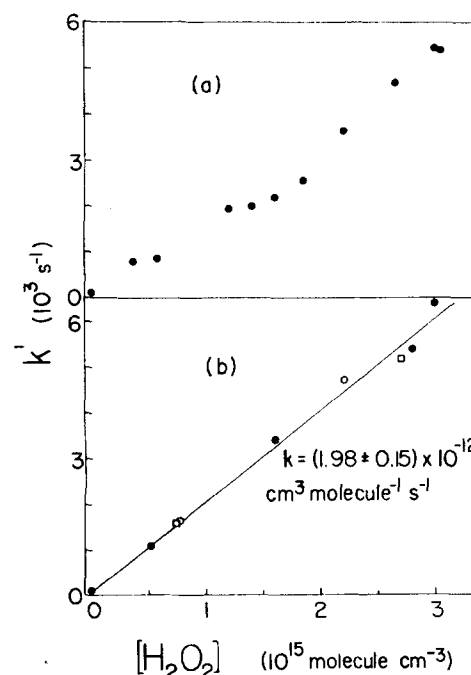


FIG. 2.  $k'$  vs  $[\text{H}_2\text{O}_2]$  data for  $T=410\text{ K}$ . (a)  $[\text{H}_2\text{O}_2]$  measured at reactor entrance, (b)  $[\text{H}_2\text{O}_2]$  measured at reactor exit.  $\bullet$ : flow rate =  $5\text{ cm s}^{-1}$ , no  $\text{O}_3$  added;  $\circ$ : flow rate =  $11\text{ cm s}^{-1}$ , no  $\text{O}_3$  added;  $\square$ : flow rate =  $11\text{ cm s}^{-1}$ ,  $\text{O}_3$  added to increase  $[\text{OH}]_0$  by a factor of 9. The solid line is obtained from an unweighted linear least squares analysis of data set (b). Data set (a) does not give a linear  $k'$  vs  $[\text{H}_2\text{O}_2]$  dependence; this is apparently the result of  $\text{H}_2\text{O}_2$  thermal decomposition in the reactor.

TABLE I. Kinetic data for the reaction  $\text{OH} + \text{H}_2\text{O}_2 \rightarrow \text{HO}_2 + \text{H}_2\text{O}$ .

$T$ (°K)	Diluent <sup>a</sup>	$[\text{H}_2\text{O}_2]$ ( $10^{15} \text{ cm}^{-3}$ )	$[\text{O}_3]$ ( $10^{15} \text{ cm}^{-3}$ )	Location of absorption cell <sup>b</sup>	Flow rate ( $\text{cm s}^{-1}$ )	$k'$ ( $\text{s}^{-1}$ )	$k_1 \pm 2\sigma^c$ ( $10^{-12} \text{ cm}^3 \text{ molecule}^{-1} \text{ s}^{-1}$ )
273	He	0	d	1	6	70	
		0.83	0			1250	
		0.94	0			1690	
		2.0	0			2990	
		2.1	0			3320	$1.50 \pm 0.16$
297	He	0	d	1	6	72	
		0.43	0		6	998	
		0.74	0		6	1600	
		1.3	0		6	2220	
		1.7 <sub>5</sub>	0		6	3020	
		2.0	0		6	3460	
		3.0	0		6	4900	
		3.2	0		6	5360	$1.59 \pm 0.08$
299	He	0	d	2	6	69	
		0.54	0		6	749	
		1.3	0		6	2190	
		1.7	0.066		6	2720	
		2.4	0		6	3760	
		3.3 <sub>5</sub>	0.14		6	5260	
		3.4	0		6	5340	$1.56 \pm 0.17$
300	$\text{SF}_6$	0	d	1	6	158	
		0.58	0		6	1070	
		1.25	0		6	2340	
		2.4	0		6	4110	
		3.6	0		6	5620	$1.53 \pm 0.13$
332	He	0	d	1	7	62	
		0.52	0		7	1040	
		1.4 <sub>5</sub>	0		7	2330	
		2.4	0		7	4150	
		2.6	0		7	4340	
		2.6	0		7	4770	
		3.4	0		7	5920	$1.72 \pm 0.12$
371	He	0	d	1	6	71	
		0.50	0		6	1040	
		0.72	0		6	1100	
		1.2	0		6	2310	
		1.6	0		6	2870	
		2.2	0		6	4550	
		2.7	0		6	4850	
		2.9	0		6	5710	$1.93 \pm 0.17$
410	He	0	d	1	5	81	
		0.52	0		5	1080	
		0.74	0.15		11	1590	
		0.77	0		11	1630	
		1.6	0		5	3400	
		2.2	0		11	4700	
		2.7	0.55		11	5140	
		2.8	0		5	5340	
		3.0	0		5	6390	$1.98 \pm 0.15$
410	He	0	d	2	6	80	
		0.36	0		6	762	
		0.57	0		6	836	
		1.2	0		6	1930	
		1.4	0		6	1990	
		1.6	0		6	2190	
		1.8 <sub>5</sub>	0		6	2560	
		2.2	0		6	3640	
		2.6 <sub>5</sub>	0		6	4680	
		3.0	0		6	5450	
		3.0 <sub>5</sub>	0		6	5360	...

<sup>a</sup>Total pressure was 100 Torr in all experiments with He diluent and 40 Torr in all experiments with  $\text{SF}_6$  diluent.<sup>b</sup>1: mixture flowed through absorption cell after leaving reactor. 2: mixture flowed through absorption cell before entering reactor.<sup>c</sup>Errors refer to precision only.<sup>d</sup>OH was produced in the absence of  $\text{H}_2\text{O}_2$  by photolyzing a mixture containing 0.5 mTorr  $\text{O}_3$ , 60 mTorr  $\text{H}_2\text{O}$ , and diluent gas.  $\text{O}_3 + h\nu (266 \text{ nm}) \rightarrow \text{O}(^1\text{D})$ ;  $\text{O}(^1\text{D}) + \text{H}_2\text{O} \rightarrow 2\text{OH}$ .<sup>e</sup>Under these experimental conditions, a nonlinear dependence of  $k'$  on  $[\text{H}_2\text{O}_2]$  was observed; this result is apparently attributable to thermal decomposition of  $\text{H}_2\text{O}_2$  during traversal from the absorption cell to the reaction zone.

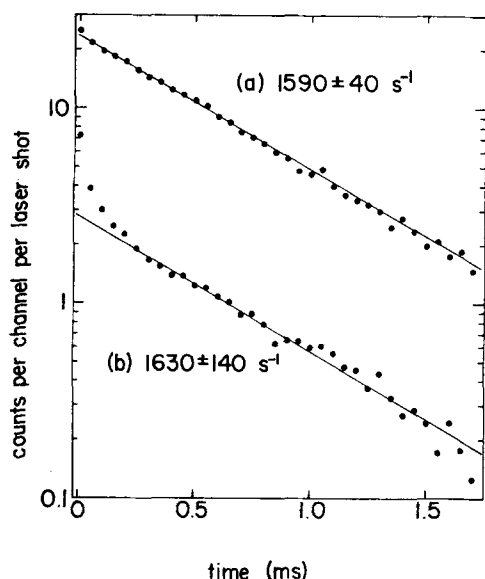


FIG. 3. Comparison of OH temporal profiles obtained in the absence and presence of added  $\text{O}_3$ . Experimental conditions:  $T=410\text{ K}$ ;  $P=100\text{ Torr (He)}$ ;  $[\text{H}_2\text{O}_2]$ ,  $[\text{O}_3]$  in units of  $10^{15}\text{ molecules cm}^{-3}$ =(a) 0.74, 0.15, (b) 0.77, 0. Number of laser shots averaged=(a) 200, (b) 1350. Solid lines are obtained from linear least squares analyses.  $k' \pm 2\sigma$  values obtained from least squares analyses are given in the figure.



The reaction of  $\text{O}(^3\text{P})$  with  $\text{H}_2\text{O}_2$  is much too slow<sup>16</sup> to produce OH on the time scale of our experiments. Since  $[\text{O}(^3\text{P})]_0$  was considerably smaller than  $[\text{OH}]_0$  and  $[\text{HO}_2]_0$  in all experiments, and since the reactions of  $\text{O}(^3\text{P})$  with OH and  $\text{HO}_2$  are not faster than Reaction (7),<sup>17,18</sup> it must be that Reaction (7) was the dominant radical-radical reaction. It is clear therefore that the presence of small amounts of  $\text{O}(^3\text{P})$  in the experiments with added  $\text{O}_3$  could not have influenced the OH decay rate.

Based on energetics,  $\text{H}_2\text{O}_2$  photolysis at 266 nm can produce OH radicals in the seven lowest vibrational levels. If a significant fraction of OH were produced vibrationally hot, and if relaxation into  $v=0$  (the only level detected by the resonance fluorescence technique), occurred on the same time scale as OH removal, underestimation of  $k'$  would result. To check for this possibility,  $k_1$  was determined at 300 K with  $\text{SF}_6$  substituted for He as the diluent gas.  $\text{SF}_6$  is an efficient vibrational relaxer for many molecules and is known to deactivate highly vibrationally excited OH ( $v \sim 9$ ) much more rapidly than He.<sup>19</sup> If vibrationally hot OH were a kinetic complication, then some change in  $k_1$  would be expected upon substitution of  $\text{SF}_6$  for Ar as the diluent gas. Within experimental error, this variation in experimental conditions had no effect on  $k_1$ . It is worth noting that  $\text{H}_2\text{O}$  is an extremely efficient vibrational relaxer for OH.<sup>20</sup>  $\text{H}_2\text{O}_2$  should also exhibit this property. Therefore, it is quite likely that any OH which was produced in excited vibrational levels was deactivated by  $\text{H}_2\text{O}_2$  and its  $\text{H}_2\text{O}$  impurity prior to reaction.

The experimental conditions employed to measure

each  $k'$  and the bimolecular rate constants derived from the  $k_1$  vs  $[\text{H}_2\text{O}_2]$  data are summarized in Table I. The  $2\sigma$  precision in the bimolecular rate constants ranges from 4%–11%. However, uncertainties in the  $\text{H}_2\text{O}_2$  absorption cross section at 228.8 nm and possible systematic errors in the absorption measurements contribute to an estimated overall accuracy of 20% (95% confidence) in the reported rate constants. An unweighted linear least squares analysis of the  $\ln k$  vs  $1/T$  data gives the following Arrhenius expression (units are  $\text{cm}^3\text{ molecule}^{-1}\text{ s}^{-1}$ ):

$$k_1 = (3.7 \pm 0.6) \times 10^{-12} \exp[-260 \pm 50/T]. \quad (\text{II})$$

The uncertainties in the above expression are  $2\sigma$  with the uncertainty in the pre-exponential factor taken to be  $2A\sigma_{\ln A}$ .

Our data agrees very well with that reported in the two recent DF-RF studies of Keyser<sup>7</sup> and Sridharan *et al.*<sup>8</sup> Apparently, all five earlier measurements of  $k_1$ <sup>1–5</sup> were in error. The complications which led to underestimation of  $k_1$  in all earlier studies have been adequately discussed elsewhere.<sup>7,8</sup> Our data and the data of Keyser and Sridharan *et al.* are plotted in Arrhenius form in Fig. 4. Sridharan *et al.* measured  $\text{H}_2\text{O}_2$  by absorption at 213 nm using an absorption cross section  $\sim 8\%$  higher than the most recently reported (and most probably correct) value.<sup>11</sup> Hence, we have scaled their results downward by 8% to allow a more direct comparison with our data. Keyser determined the  $\text{H}_2\text{O}_2$  concentration by absorption at 199.5 nm using a cross section which he measured; since his cross section agreed with the one reported by Molina and Molina<sup>11</sup> to within 2% and since systematic errors often cancel out when the concentration measurement is carried out in the same system as the cross section measurement, his data are plotted as reported. The solid line in Fig. 4 is the Arrhenius line determined using only our data

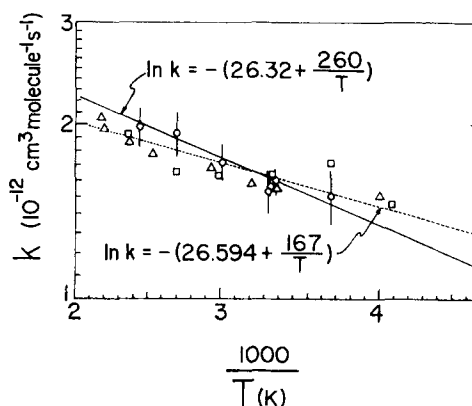


FIG. 4. Arrhenius plot of our data (○) and the data of Keyser (□) and Sridharan *et al.* (Δ). The data of Sridharan *et al.* are scaled downward by 8% as discussed in the text. The solid line is obtained from an unweighted linear least squares analysis of our data only. The dotted line is obtained from an unweighted linear least squares analysis of all data. For clarity,  $2\sigma$  error bars are given only for our data; the error bars represent precision only. Arrhenius expressions given in the figure are in units of  $\text{cm}^3\text{ molecule}^{-1}\text{ s}^{-1}$ .

while the dotted line is obtained from an unweighted linear least squares analysis of data from all three investigations. The expression obtained by averaging the results of all three studies is (units are  $\text{cm}^3 \text{ molecule}^{-1} \text{ s}^{-1}$ )

$$k_1 = (2.82 \pm 0.30) \times 10^{-12} \exp[-(167 \pm 35)/T]. \quad (\text{III})$$

We measure a slightly larger activation energy than was obtained in either DF-RF study, so extrapolation of our results to lower stratospheric temperatures (210–240 K) gives rate constants about 10%–15% lower than those obtained when data from all three studies are averaged. This difference, however, easily falls within the combined error limits of the three investigations.

## ACKNOWLEDGMENT

This work was supported by NASA through subcontract (954814) from the Jet Propulsion Laboratory.

<sup>1</sup>N. R. Greiner, *J. Phys. Chem.* **72**, 406 (1968).

<sup>2</sup>R. A. Gorse and D. H. Volman, *J. Photochem.* **1**, 1 (1972).

<sup>3</sup>J. F. Meagher and J. Heicklen, *J. Photochem.* **3**, 455 (1975).

<sup>4</sup>W. Hack, K. Hoyerman, and H. Gg. Wagner, *Int. J. Chem. Kinet. Symp.* **1**, 329 (1975).

<sup>5</sup>G. W. Harris and J. N. Pitts, Jr., *J. Chem. Phys.* **70**, 2581 (1979).

<sup>6</sup>*The Stratosphere: Present and Future*, edited by R. D. Hudson and E. I. Reed (NASA reference publication 1049, 1979).

<sup>7</sup>L. F. Keyser, *J. Phys. Chem.* **84**, 1659 (1980).

<sup>8</sup>U. C. Sridharan, B. Reimann, and F. Kaufman, *J. Chem. Phys.* **73**, 1286 (1980).

<sup>9</sup>P. H. Wine, N. M. Kreutter, and A. R. Ravishankara, *J. Phys. Chem.* **83**, 3191 (1979), and references therein.

<sup>10</sup>P. H. Wine, A. R. Ravishankara, N. M. Kreutter, R. C. Shah, J. M. Nicovich, R. L. Thompson, and D. J. Wuebbles, *J. Geophys. Res.* **86**, 1105 (1981).

<sup>11</sup>L. T. Molina and M. J. Molina, *J. Photochem.* **15**, 97 (1981).

<sup>12</sup>N. R. Greiner, *J. Chem. Phys.* **45**, 99 (1966).

<sup>13</sup>L. J. Stief and V. J. DeCarlo, *J. Chem. Phys.* **50**, 1234 (1969).

<sup>14</sup>J. C. Brock and R. T. Watson, *Chem. Phys. Lett.* **71**, 371 (1980).

<sup>15</sup>I. S. Fletcher and D. Husain, *Can. J. Chem.* **54**, 1765 (1976).

<sup>16</sup>D. D. Davis, S. Fischer, and R. Schiff, *J. Chem. Phys.* **61**, 2213 (1974).

<sup>17</sup>R. S. Lewis and R. T. Watson, *J. Phys. Chem.* **84**, 3495 (1980).

<sup>18</sup>W. Hack, A. W. Preuss, F. Temps, and H. Gg. Wagner, *Ber. Bunsenges. Phys. Chem.* **83**, 1275 (1979).

<sup>19</sup>J. A. Davidson, C. M. Sadowski, H. I. Schiff, G. E. Streit, C. J. Howard, D. A. Jennings, and A. L. Schmeltekopf, *J. Chem. Phys.* **64**, 57 (1976).

<sup>20</sup>A. R. Ravishankara, P. H. Wine, and A. O. Langford, *J. Chem. Phys.* **70**, 984 (1979), and references therein.